A comparison of $N_e(h)$ model profiles with ground-based and topside sounder observations

Andrei V. Mikhailov (1), **Tatjana Yu. Leschinskaya** (1), **Gloria Miro** (2) **and Victor Kh. Depuev** (1)
(1) *Institute of Terrestrial Magnetism, Ionosphere and Radio Wave Propagation, Russian Academy of Sciences, Troitsk, Moscow Region, Russia*
(2) *National Institute of Aerospace Technology, Mazagón (Huelva), Spain*

Abstract
Monthly median empirical models IRI-95 and NeUoG were compared with incoherent scatter EISCAT and Millstone Hill observations as well as with El Arenosillo Digisonde $N_e(h)$ bottomside profiles. A comparison was made for various seasons, levels of solar activity, daytime and night-time hours. The results on the topside comparison: 1) the IRI-95 model systematically and strongly overestimates the $N_e(h)$ effective scale height both for daytime and night-time periods especially during maximum and middle solar activity both at EISCAT and Millstone Hill; 2) the NeUoG model on the contrary systematically underestimates the scale height at all levels of solar activity. But the NeUoG model provides much better overall agreement with SD being less by a factor of 1.5-1.7 in comparison with the IRI-95 model results. The results on the bottom-side comparison: 1) the IRI-95 accuracy is different for daytime and night-time hours, being much worse for the night-time; 2) the NeUoG model similar to IRI-95 demonstrates much worse accuracy for the night-time hours; 3) the NeUoG model demonstrates no advantages over the IRI-95 model in the bottomside $N_e(h)$ description. A new simple TopN_e model for the $N_e(h)$ topside distribution based on the EISCAT and Millstone Hill observations is proposed. The model is supposed to be normalized by the observed hmF_2 and NmF_2 values and is valid below a 600 km height. The TopN_e model provides good approximation accuracy over EISCAT and Millstone Hill observations. A comparison with the independent Intercosmos-19 topside sounder observations is given.

Key words *empirical $N_e(h)$ models – incoherent scatter – digisonde – topside sounder observations*

1. Introduction

Knowledge of electron density height distribution $N_e(h)$ is of great importance for ground-based and space techniques using radio signals traveling through the ionosphere. The $N_e(h)$ profiles in the most widely used IRI model (IRI-80, 86, 90, 95) are based on the bottom- and topside ionosonde observations.

If the bottomside $N_e(h)$ model description has been improved over the years, the topside $N_e(h)$ is based on Alouette 1 and 2 topside sounder measurements from 1962 to 1966 and practically has not been changed since 1970 when it was proposed by Bent and colleagues (see Bilitza *et al.*, 1993 and references therein). These Alouette observations include only solar minimum and low solar moderate ($F_{10.7} < 130$) conditions. Obviously this shortcoming of the IRI topside $N_e(h)$ was revealed in comparison with direct incoherent scatter (Buonsanto, 1989) and Intercosmos-19 topside sounder observations

Mailing address: Prof. Andrei V. Mikhailov, Institute of Terrestrial Magnetism, Ionosphere and Radio Wave Propagation, Russian Academy of Sciences, 142092 Troitsk, Moscow Region, Russia. e-mail: avm71@orc.ru

(Benjkova *et al.*, 1990). So additional attempts have been undertaken to improve the IRI model $N_e(h)$ specification (Decker *et al.*, 1997). Recently a new global University of Graz $N_e(h)$ model (NeUoG model) has been proposed by Leitinger (1998) in the framework of the European COST 238/251 Projects.

The only straightforward way to estimate the quality of the $N_e(h)$ model is to compare the $N_e(h)$ model profiles with direct incoherent scatter or topside ionospheric sounder observations. A comparison with TEC is also possible (Bilitza *et al.*, 1998), but TEC is an integral characteristic and does not say anything about the specific shortcomings of the $N_e(h)$ distribution.

The aim of this paper is to compare the IRI-95 and the NeUoG-model with incoherent scatter EISCAT (69.6N; 19.2E) and Millstone Hill (42.6N; 288.5E) as well as with El Arenosillo (37.1N; 353.3E) digisonde observations for different geophysical conditions to make a quantitative conclusion about the merits of these models. A new TopN_e model for the $N_e(h)$ topside specification based on the EISCAT and Millstone Hill observations is proposed as well and some comparisons with Intercosmos-19 topside sounder observations are made.

2. Data selection

Daytime (around noon) and nighttime (around midnight) EISCAT and Millstone Hill incoherent scatter observations were chosen for the analysis. EISCAT summer nighttime hours in fact correspond to twilight conditions as solar zenith angle is around 90°. Periods of maximum, middle and low solar activity were analyzed. Only quiet days with $A_p < 12$ were selected. The use of quiet time periods implies the analyzed conditions to be close to monthly median as the tested models are monthly median ones. Additional comparison of model bottomside $N_e(h)$ was made with available daytime El Arenosillo digisonde observations for solar middle and minimum conditions. The nighttime digisonde profiles were not analyzed as there is a great deal of uncertainty with the $N_e(h)$ specification in the *E-F* valley region, especially during night-time hours. The distribution of tested data over years, solar activity and seasons is given in table I.

The EISCAT CP-1 program provides range profiles of N_e every 5 min with the antenna beam directed along the local geomagnetic field line. As the field line inclination at the EISCAT location is 77.6° and $\sin I = 0.98$, these range profiles may be considered with sufficient accuracy as height $N_e(h)$ profiles. They were used to calculate median profiles over a two-hour time interval (about 25 values) for the chosen periods. These median $N_e(h)$ profiles were compared with model $N_e(h)$ for corresponding geophysical conditions.

Millstone Hill IS facility provides three local $N_e(h)$ profiles per hour, and we used at least a 3 h period of observation (8-10 profiles) to calculate median height profiles. Of course, such a 3 h averaging interval is too long with respect to the 1.5 h characteristic time for the daytime F_2-layer maximum, so we tried to select the days and periods around noon and midnight of relative stability in NmF_2 and hmF_2 daily variations. These median $N_e(h)$ profiles were spline-interpolated to give a constant 10 km height step convenient for a comparison with the models.

Routine El Arenosillo digisonde daytime $N_e(h)$ profiles obtained with a 10 km height step were used for a comparison. Each $N_e(h)$ was analyzed separately and only reliable profiles for quiet days ($A_p < 12$) were left for further comparison. The tested models were normalized by the observed NmF_2 and hmF_2 values to analyze the relative accuracy of model $N_e(h)$ specification. We calculated the standard deviation (SD) and the mean shift (SHIFT) of model $\log Ne(h)$ with respect to the observed $\log Ne(h)$ for the topside and bottomside of $N_e(h)$ separately using the following expressions:

$$\mathrm{SHIFT} = \frac{1}{n}\sum dX$$

$$\mathrm{SD} = \sqrt{\frac{1}{(n-1)}\left[\sum (dX^2) - \frac{1}{n}\left(\sum dX\right)^2\right]}$$

where $dX = \log N_{emod} - \log N_{eobs}$ at each height step. The SHIFT parameter gives mainly the qualitative characteristic of the model $N_e(h)$ pro-

Table I. The distribution of testing data over years, solar activity levels and seasons for EISCAT, Millstone Hill and El Arenosillo observations.

Solar activity level	Years	Average $F_{10.7}$	Season	Number of profiles used
		EISCAT		
Maximum	1989-1991	190-222	Winter Summer Equinox	23
Middle	1987,1988,1992	123-153	Summer Equinox	18
Minimum	1987	77-83	Summer Equinox	10
		Millstone Hill		
Maximum	1990-1991	184-215	Equinox Winter	18
Middle	1992-1993	124-134	Summer Winter	11
Minimum	1997	73	Winter	6
		El Arenosillo		
Middle	1993	108.7	Equinox Summer Winter	37
Minimum	1995-1996	65-73	Equinox Summer Winter	59

Table II. Empirically found correction factors for H_p to fit the observed H_{eff} at Millstone Hill.

Solar activity level	Daytime	Night-time
Maximum	0.65	1.0
Middle	0.85	1.15
Low	1.1	1.25

file with respect to the observed one, while the standard deviation SD gives the quantitative characteristic of such a comparison. Calculated SHIFT and SD over each profile with a 10 km height step were averaged for given solar activity level, day and night periods. The results of this comparison for three models in the 150-600 km height range for EISCAT and Millstone Hill observations are given in tables III and IV. Table IV also gives the results for El Arenosillo digisonde bottomside noon $N_e(h)$ observations.

3. TopN_e model derivation

Incoherent scatter observations are known to provide an excellent material on $N_e(h)$, $T_e(h)$, $T_i(h)$ height distribution for 1-2 decades of continuous observations for all seasons and local times. But unlike satellite observations, they provide only local data. These IS observations may be used for the analysis and derivation of $N_e(h)$ models, but being linked to local observations such models need special testing to check

Table III. Model testing results for topside $N_e(h)$. Mean SD and (SHIFT) values are given for daytime and night-time (second line) periods for three levels of solar activity.

Solar activity level	IRI-95	NeUoG-model	TopN_e-model
		EISCAT	
Maximum	0.125 (0.178)	0.059 (– 0.085)	0.012 (0.021)
	0.079 (0.098)	0.035 (– 0.029)	0.014 (– 0.009)
Middle	0.051 (0.095)	0.047 (– 0.077)	0.019 (0.029)
	0.041 (0.071)	0.044 (– 0.027)	0.026 (0.027)
Minimum	0.064 (0.022)	0.025 (– 0.035)	0.023 (0.033)
	0.046 (0.037)	0.053 (– 0.051)	0.030 (0.041)
Average SD daytime	0.080	0.044	0.018
Average SD night-time	0.055	0.044	0.023
		Millstone Hill	
Maximum	0.095 (0.155)	0.046 (– 0.019)	0.025 (0.000)
	0.117 (0.152)	0.057 (0.071)	0.021 (0.010)
Middle	0.055 (0.111)	0.024 (– 0.032)	0.016 (0.021)
	0.061 (0.086)	0.036 (– 0.000)	0.033 (– 0.014)
Minimum	0.066 (0.126)	0.031 (0.047)	0.034 (– 0.025)
	0.039 (0.001)	0.051 (– 0.055)	0.032 (– 0.016)
Average SD daytime	0.072	0.034	0.025
Average SD night-time	0.072	0.048	0.029

their applicability to other areas over the globe. A simple empirical model of the topside $N_e(h)$ distribution based on the analysis of EISCAT (auroral zone) and Millstone Hill (midlatitude) observations is proposed. The approximation accuracy of the experimental IS profiles with this model is analyzed and topside sounder Intercosmos-19 $N_e(h)$ observations are used as an independent material for comparison.

The analysis of the observed IS $N_e(h)$ profiles shows that the $N_e(h)$ topside distribution below 600 km has practically constant effective scale height. General expression for the vertical plasma velocity in the ambipolar approximation is following (Banks and Kockarts, 1973)

$$V_z = -\frac{k(T_e + T_i)}{m_i \nu_i} \sin^2 I \cdot \left[\frac{d \ln N_e}{dh} + \frac{g m_i}{k(T_e + T_i)} + \frac{d \ln (T_e + T_i)}{dh} \right] + W \tag{3.1}$$

where V_z is the vertical plasma velocity, T_e and T_i - plasma temperatures, m_i - O^+ ion mass, ν_i - total O^+ ions collision frequency, W - vertical plasma drift velocity due to thermospheric winds and electric fields. The expression (3.1) may be rewritten to give the effective scale height, $H_{\text{eff}} = -[d \ln N_e / dh]^{-1}$

$$H_{\text{eff}} = \left[\frac{V_z - W}{D_a} + \frac{g m_i}{k(T_e + T_i)} + \frac{d \ln (T_e + T_i)}{dh} \right]^{-1} \tag{3.2}$$

where $D_a = k(T_e + T_i) \sin^2 I / m_i \nu_i$ is the ambipolar diffusion coefficient.

The second term in (3.2) is known to provide the main contribution to H_{eff}. The quantitative contribution of different terms to H_{eff} in (3.2) may be estimated using the results of the self-consistent method by Mikhailov and Schlegel (1997) application to the incoherent scatter observations. This method using the standard $N_e(h)$,

Table IV. Model testing results for bottomside $N_e(h)$. Mean SD and (SHIFT) values are given for daytime and night-time (second line) periods for three (EISCAT, Millstone Hill) and two (El Arenosillo) levels of solar activity. Only noon El Arenosillo observations are analyzed.

Solar activity level	IRI-95	NeUoG-model
	EISCAT	
Maximum	0.066 (– 0.019)	0.079 (0.000)
	0.333 (– 0.326)	0.162 (– 0.240)
Middle	0.040 (0.011)	0.066 (– 0.025)
	0.461 (– 0.397)	0.127 (– 0.212)
Minimum	0.032 (– 0.012)	0.102 (– 0.043)
	0.184 (– 0.197)	0.137 (0.002)
Average SD daytime	0.046	0.082
Average SD night-time	0.326	0.142
	Millstone Hill	
Maximum	0.129 (– 0.044)	0.114 (– 0.046)
	0.194 (0.012)	0.372 (0.169)
Middle	0.066 (– 0.038)	0.064 (– 0.040)
	0.240 (– 0.084)	0.315 (0.121)
Minimum	0.086 (– 0.076)	0.097 (– 0.164)
	0.238 (– 0.029)	0.273 (0.136)
Average SD daytime	0.094	0.092
Average SD night-time	0.224	0.320
	El Arenosillo	
Middle	0.092 (– 0.062)	0.198 (– 0.123)
Minimum	0.079 (– 0.020)	0.270 (– 0.190)
Average SD daytime	0.085	0.234

$T_e(h)$, $T_i(h)$, $V_i(h)$ incoherent scatter observations provides the set of main aeronomic parameters responsible for the observed $N_e(h)$ distribution in the daytime F_2-region. The calculated neutral composition and temperature as well as vertical plasma drift W allows us to estimate the contribution of different terms in (3.2) to H_{eff}. Figure 1 gives two examples of such $N_e(h)$ fitting analysis for daytime hours and the ratios of the first and the third terms in (3.2) to the second one. The contribution of the first term is seen to decrease rapidly with height, then remains practically unchanged above the hmF_2 height. The contribution of the third term may be up to 30% in the topside. The contribution of the first term is seen to increase at lower latitudes where the magnetic inclination I is less. This is due to D_a dependence on $\sin^2 I$ as well as to W increase being related to the meridional thermospheric wind V_n as $W = V_n \sin I \cos I$. Therefore, in principle, with known plasma temperatures $T_e(h)$ and $T_i(h)$ the effective scale height H_{eff} may be calculated above 400-450 km using plasma scale height H_p corrected by a factor of ± (10-15)% (the first term contribution). This correction factor is negative during daytime and positive during night-time hours. Both the northward thermospheric wind (negative plasma drift W) and the upward plasmaspheric flux decrease H_{eff} with respect to H_p during the daytime. The effect of winds and plasmaspheric fluxes is inverse during night-time hours and H_{eff} increases with re-

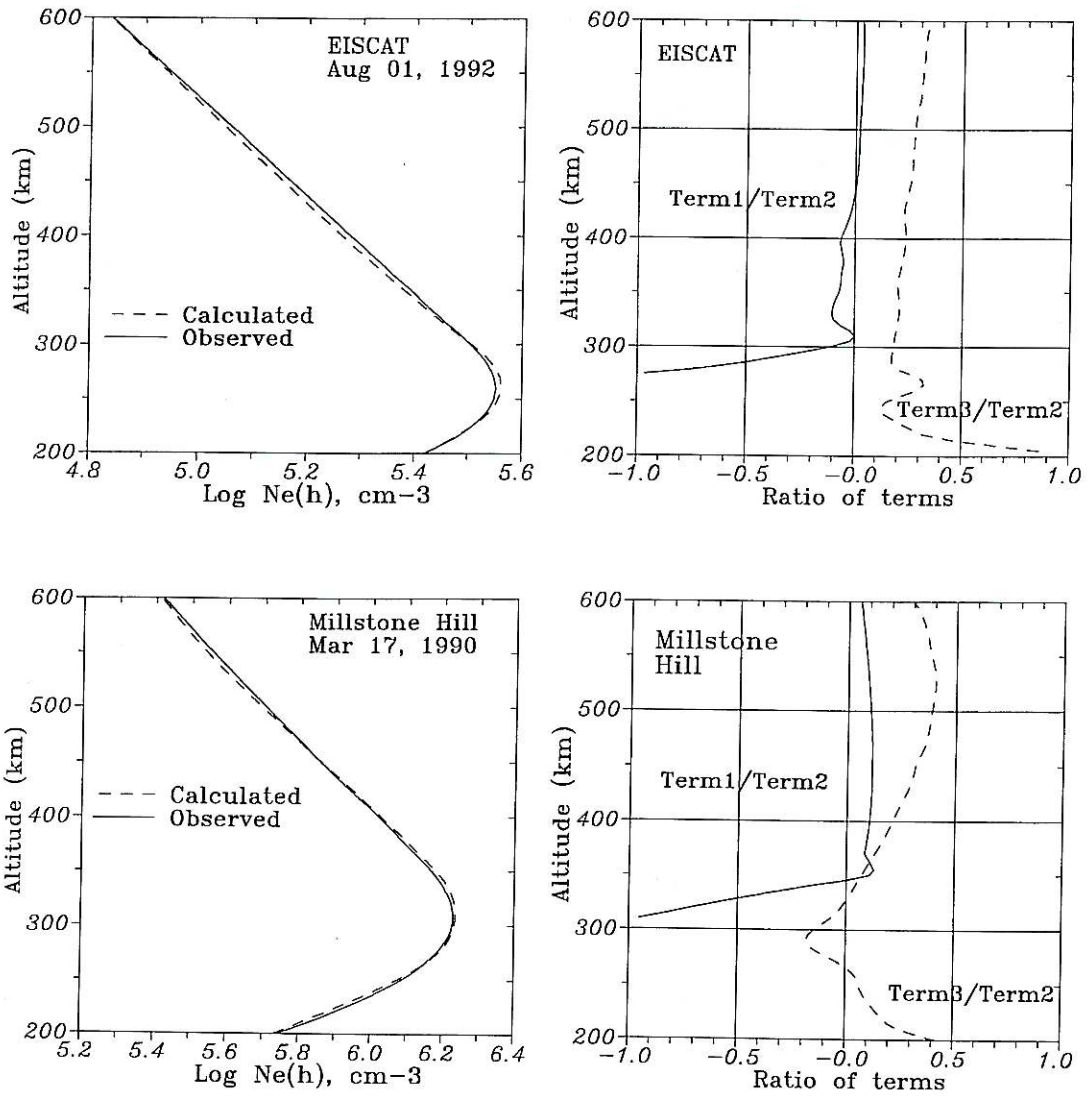

Fig. 1. The results of $N_e(h)$ fitting for EISCAT and Millstone Hill observations using the Mikhailov and Schlegel (1997) self-consistent method (left boxes) and corresponding height variations for Term1/Term2 and Term3/Term2 ratios from the expression (3.2).

spect to H_p (Ivanov-Kholodny and Mikhailov, 1986).

The most essential point is to use correct plasma temperatures. As the model is supposed to be used globally at medium and moderately high latitudes, the global T_e and T_i model should be applied. The Brace and Theis (1981) model for T_e and the Titheridge (1998) model for T_i were used in model derivation. Unfortunately, a comparison of model T_e with direct IS observations gives large discrepancies, therefore such a simple H_p correction cannot be applied directly.

Usually model T_e are much higher than the observed ones and a special analysis was undertaken to find empirical factors to correct the calculated plasma scale height. On the other hand, T_i being linked to the neutral temperature (MSIS-83 model was used in our analysis) in the considered height range, turns out to be close to IS observations. The empirical factors for H_p turned our to be larger than mentioned above to compensate improper model T_e values. Moreover a different correction was required for different levels of solar activity and seasons. Table II gives the empirical correction factors for H_p to fit the Millstone Hill $N_e(h)$ observations. The above mentioned tendency in daily H_{eff} variations due to thermospheric wind and plasmaspheric flux changes is clearly seen in table II. Somewhat different coefficients were obtained to fit the EISCAT observations keeping in mind specific conditions of the auroral ionosphere especially during winter time.

Chapman shape profile was used to model $N_e(h)$ in the vicinity of the F_2-layer maximum

$$N_e(h) = N_m \exp[1 - X - \exp(-X)] \qquad (3.3)$$

where $X = (h\text{-}h_m)/H_{Ch}$ and H_{Ch} is a scale height to be specified. After differentiation (3.3) gives

$$\frac{d \ln N_e}{dh} = -\frac{1}{H_{Ch}} + \frac{\exp(-X)}{H_{Ch}}. \qquad (3.4)$$

The scale height H_{Ch} is specified under the condition $h\text{-}h_m = H_{Ch}$. Keeping in mind that $d \ln N_e/dh = -1/H_{eff}$, we obtain from (3.4) $H_{Ch} = 0.632\ H_{eff}(h_1)$. The H_{eff} is taken at the level $h_1 = h_m + H_{eff}(h_2)$. Usually $h_2 = 375$ km, but $h_2 = 475$ km for daytime at high solar activity. Linear interpolation is applied everywhere to find the parameters for twilight and intermediate levels of solar activity.

The $N_e(h)$ height distribution above the h_1 level is obtained by the $1/H_{eff}$ integration in height

$$N_e(h) = N_e(h_1) \exp\left(-\int_{h_1}^{h} \frac{dz}{H_{eff}}\right). \qquad (3.5)$$

Further analysis has shown that better $N_e(h)$ approximation for EISCAT and Millstone Hill observations for all conditions except for solar minimum may be obtained if a constant H_{eff} is applied above the $h_c = h_m + H_n(h_m)$ height, H_n being the neutral scale height for atomic oxygen at the F_2-layer maximum and $H_{eff} = -(d \ln N_e/dh)^{-1}$ is the scale height around 450 km obtained from (3.5).

4. Comparison with observations

The results of IRI-95 and NeUoG models testing are given for topside (table III) and bottomside (table IV) $N_e(h)$ observed with EISCAT and Millstone Hill IS facilities. A similar comparison was made for the newly proposed TopN_e model to demonstrate the accuracy of data approximation with this model. Table IV also gives the results for IRI-95 and NeUoG models comparison with noon El Arenosillo digisonde $N_e(h)$ observations.

Examples of typical (with SD and SHIFT close to the values given in tables III and IV) model $N_e(h)$ profiles along with the IS observations are shown in figs. 2 and 3 for day and night-time periods and three levels of solar activity. Figure 4 gives a comparison with digisonde daytime observations for three seasons, middle and low solar activity. Model profiles are normalized by the observed hmF_2 and NmF_2 values.

5. Discussion and conclusions

The results of the topside $N_e(h)$ comparison (table III, also figs. 2 and 3) show:

1) The IRI-95 model systematically and strongly overestimates the scale height (positive SHIFT) both for daytime and night-time periods especially during maximum and medium solar activity. This is not surprising as the Allouette 1 and 2 observations at low solar activity were used for the IRI model derivation. Average SD are quite large (0.06-0.08) being close for daytime and night-time periods. These conclusions are valid both for EISCAT and Millstone Hill.

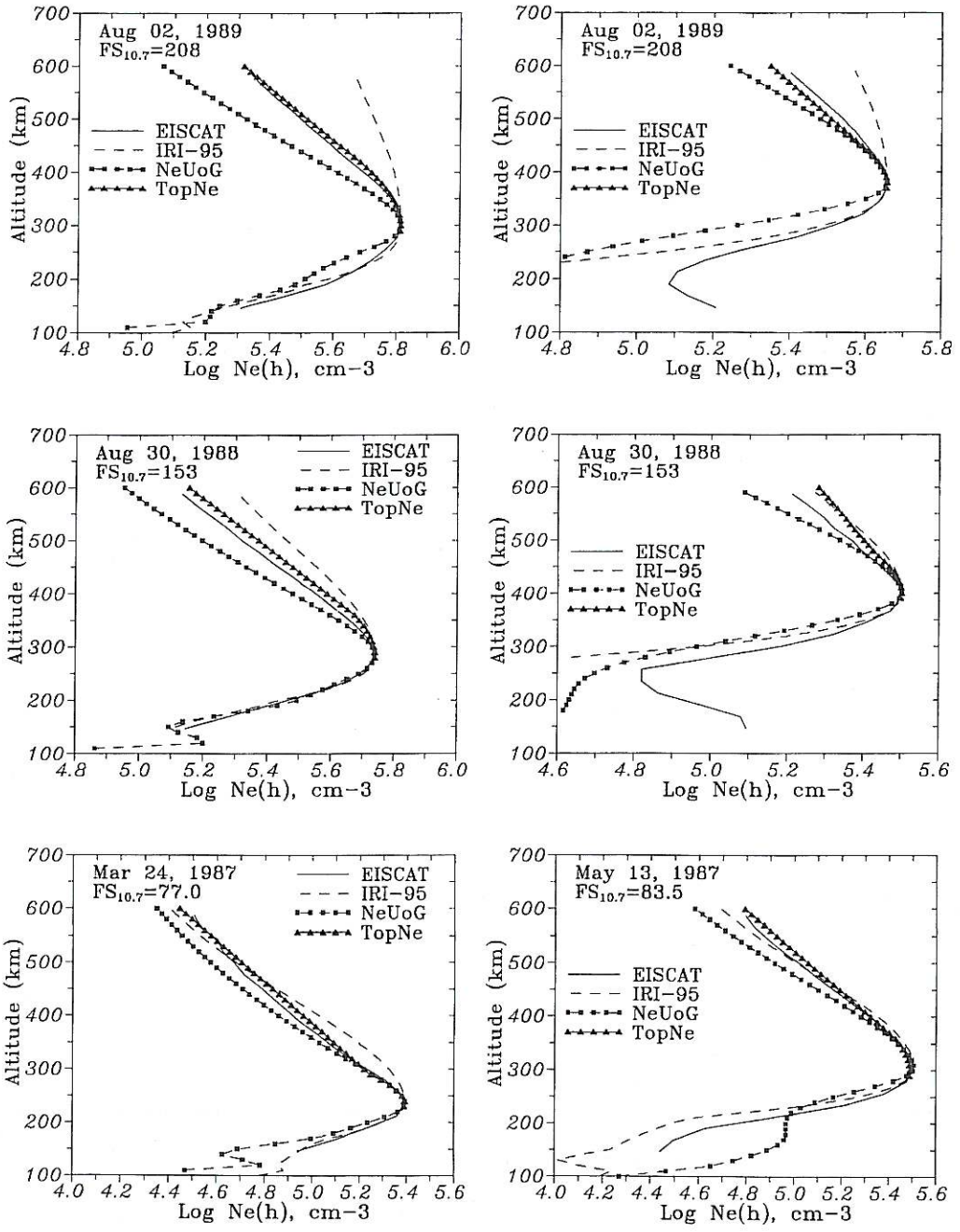

Fig. 2. Typical model $N_e(h)$ profiles along with the EISCAT observations for day (left hand boxes) and night (right hand boxes) periods for maximum, middle and low levels of solar activity. Model $N_e(h)$ profiles are normalized by the observed hmF_2 and NmF_2.

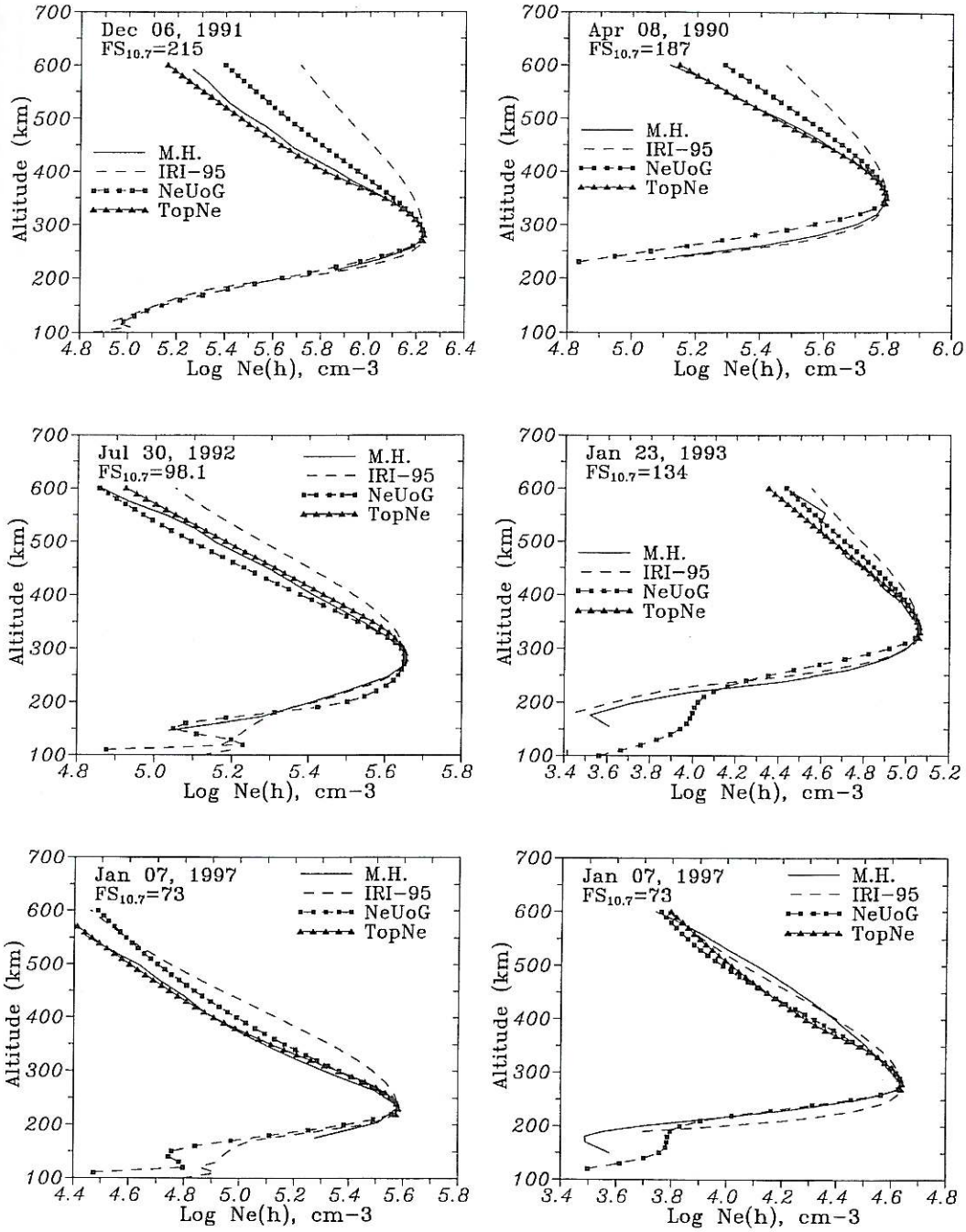

Fig. 3. Same as fig. 2, but for Millstone Hill observations.

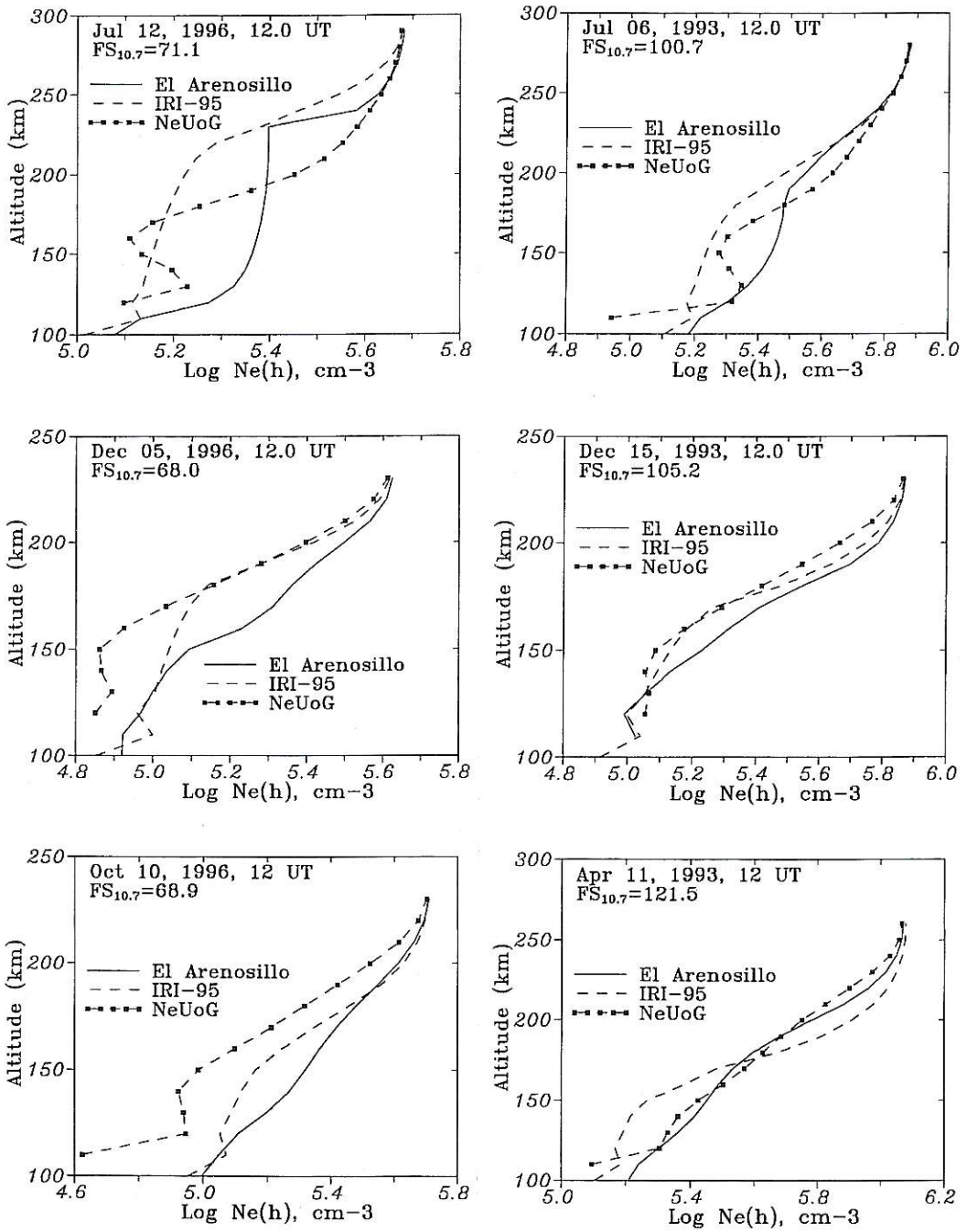

Fig. 4. A comparison of typical El Arenosillo digisonde noon-time $N_e(h)$ profiles with the IRI-95 and NeUoG models for middle and low of solar activity.

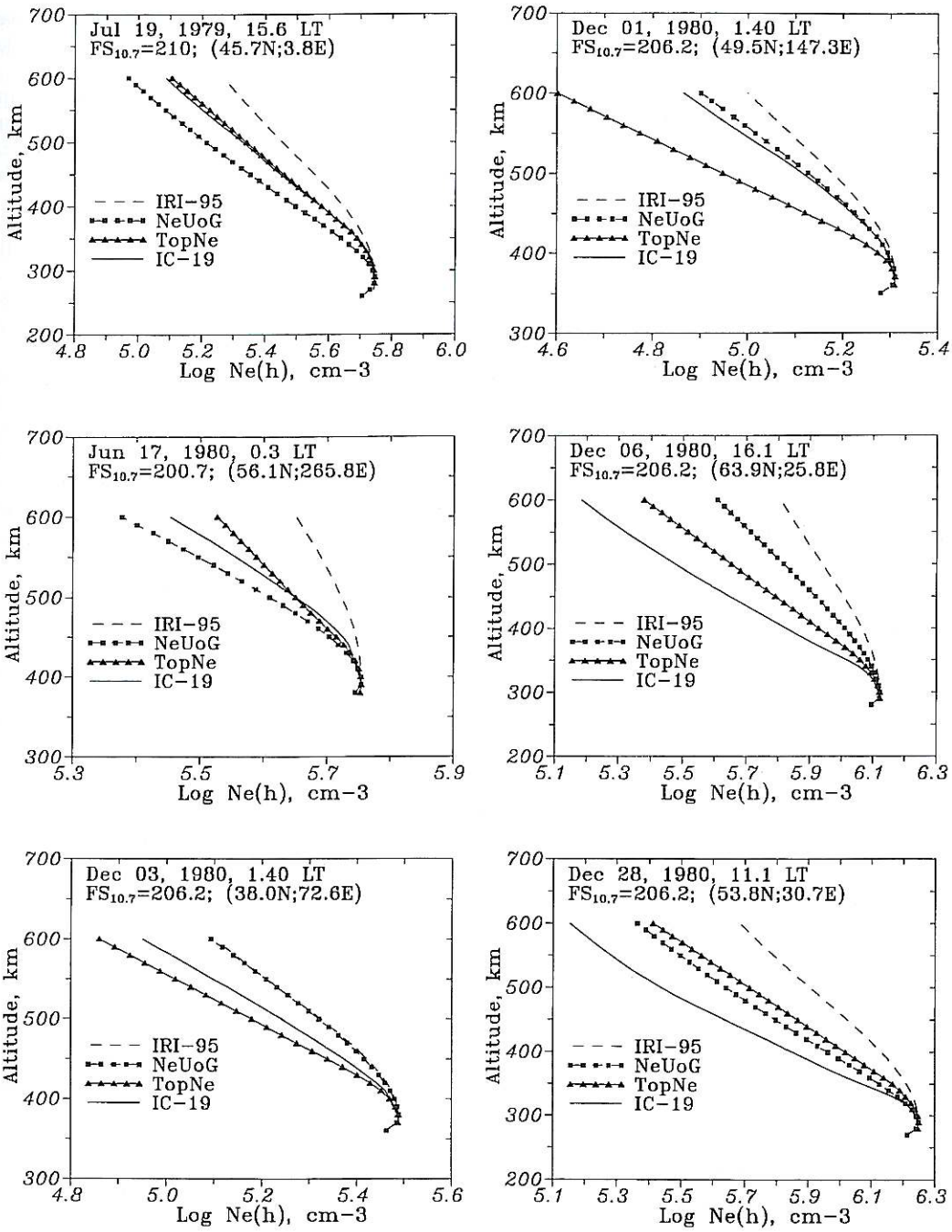

Fig. 5. A comparison of three models with the Intercosmos-19 topside sounder observations. Model $N_e(h)$ profiles are normalized by the observed hmF_2 and NmF_2 values.

2) The NeUoG-model, on the contrary systematically underestimates the scale height (negative SHIFT) at all levels of solar activity. This effect is especially obvious in comparison with EISCAT observations. No noticeable difference is seen between daytime and night-time conditions – the SD is about 0.035-0.045. But this is much less (by a factor of 1.5-1.7) than the IRI-95 model. So, the NeUoG model is much more efficient than IRI-95 in describing the $N_e(h)$ topside distribution.

3) A new TopN_e-model provides quite good approximation accuracy. The SD ranges from 0.018 to 0.029 and this is by a factor of 2.7-3.2 smaller than the IRI-95 model gives. No systematic shift of the scale height is seen – half of the results has one sign, the other has the opposite. But it should be kept in mind that the TopN_e model was derived using the same IS observations. A comparison with the independent topside sounder Intercosmos-19 observations is given below in fig. 5.

The results on the bottomside comparison (table IV, also figs. 2 to 4) show:

1) Unlike the topside case the IRI-95 bottomside description accuracy is quite different for daytime and night-time hours. It is much worse for the night-time period where the average SD equals 0.326 at EISCAT and 0.224 at Millstone Hill. During the daytime SD is quite acceptable being equal to 0.046 at EISCAT, 0.094 at Millstone Hill and 0.086 at El Arenosillo. Negative SHIFT at EISCAT and Millstone Hill tells that the IRI-95 bottomside $N_e(h)$ profile is narrower (especially during night-time) than the observed one. This is the case for all levels of solar activity at both IS locations. At El Arenosillo the sign of SHIFT is also negative telling us that the IRI-95 profile is narrower than the observations.

2) The NeUoG model does not show any systematic shift of the $N_e(h)$ profile (signs of SHIFT are different), but similar to the IRI-95 model the accuracy of the night-time $N_e(h)$ description is much worse (SD = 0.142-0.32) compared to the daytime period (SD = 0.082-0.092). Even worse results are obtained in comparison with digisonde observations. Average daytime SD = 0.235 and this is worse than the IRI-95 model provides. So one cannot say that the NeUoG model demonstrates any advantages over the IRI-95 model in the bottomside $N_e(h)$ description.

On the other hand, fig. 4 shows the problems with the digisonde $N_e(h)$ profile during daytime solar minimum conditions. Figure 4 (top left hand panel) obviously shows the effect of the well developed F_1-layer appearance. The automatic ionogram scaling results in an unrealistic $N_e(h)$ profile. An analysis of the El Arenosillo digisonde $N_e(h)$ profiles shows that this is a typical daytime situation at solar minimum. Obviously a comparison of models with such $N_e(h)$ profiles is not correct.

A newly developed TopN_e model may be compared with Intercosmos-19 topside sounder observations which were not used for the model derivation. The Intercosmos-19 sounder operated during very high solar activity (1979-1980). Some winter and summer, daytime and night-time $N_e(h)$ profiles obtained in different longitudinal sectors were chosen for a comparison. Three models were compared with the observed $N_e(h)$ profiles in fig. 5. As above, model profiles were normalized by the observed hmF_2 and NmF_2 values. Left-hand boxes are supposed to demonstrate more or less close agreement of the TopN_e model with the observations, while right-hand boxes give the examples of poorer agreement. As in figs. 2 and 3 the IRI-95 model is very far from the observations in all cases while the NeUoG model gives much better overall agreement.

Three December cases (right-hand boxes) were specially chosen to demonstrate the problems with a pure empirical approach to the $N_e(h)$ modeling. Dynamical effects related to the thermospheric winds and the plasmaspheric fluxes are clearly seen in the $N_e(h)$ topside distributions. Strong poleward neutral thermospheric wind along with the upward plasmaspheric flux result in a small H_{eff} during daytime winter hours on December 6 and December 28. The opposite effect is seen for the night-time case of December 1, but not for similar conditions on December 3 (left-hand, bottom box). Obviously it is a problem to take into account such longitudinal variations in an empirical model. A more extended comparison of the TopN_e model with topside sounder observations is required in fu-

ture to obtain statistically significant figures of merit. But the most perspective solution is seen in a semi-empirical approach to the $N_e(h)$ modeling when observed hmF_2 and NmF_2 values are included in a theoretical model to give a proper $N_e(h)$ description.

Acknowledgements

The authors thank the Director and the staff of EISCAT for running the radar and providing the data. The EISCAT Scientific Association is funded by scientific agencies of Finland (SA), France (CNRS), Germany (MPG), Norway (NF), Sweden (NFR), and the United Kingdom (PPARC), we are also grateful to John Foster and the Millstone Hill Group of the Massachusetts Institute of Technology, Westford, for providing the data.

REFERENCES

BANKS, P.M. and G. KOCKARTS (1973): *Aeronomy* (Academic Press, New York, London), p. 164.

BENJKOVA, N.P., P.V. KISHCHA, E.F. KOZLOV, N.A. KOCHENOVA, N.I. SAMOROKIN and M.D. FLIGEL (1990): The topside ionosphere profiles and their modelling, *Geomagn. Aeron.*, **30**, 945-947 (in Russian).

BILITZA, D., K. RAWER, L. BOSSY and T. GULYAEVA (1993): International reference ionosphere-past, present, and future: I. Electron density, *Adv. Space Res.*, **13** (3), 3-13.

BRACE, L.H. and R.F. THEIS (1981): Global empirical models of ionospheric electron temperature in the upper *F*-region and plasmasphere based on *in situ* measurements from Atmospheric Explorer-C, ISI-1 and ISI-2 satellites, *J. Atmos. Terr. Phys.*, **43**, 1317-1343.

BUONSANTO, M.J. (1989): Comparison of incoherent scatter observations of electron density, and electron and ion temperature at Millstone Hill with the International Ionosphere, *J. Atmos. Terr. Phys.*, **51**, 441-468.

DECKER, D.T., D.N. ANDERSON and A.J. PREBLE (1997): Improving IRI-90 low-latitude electron density specification, *Radio Sci.*, **5**, 2003-2019.

IVANOV-KHOLODNY, G.S. and A.V. MIKHAILOV (1986): *The Prediction of Ionospheric Conditions* (D. Reidel, Dordrecht, Holland), p. 46.

LEITINGER, R. (1998): NeUoG-plas-an easy to use global electron density model for the ionosphere and the plasmasphere, in *Proceedings of the 2nd COST 251 Workshop, 30-31 March 1998, Side, Turkey*, 140-150.

MIKHAILOV, A.V. and K. SCHLEGEL (1997): Self-consistent modelling of the daytime electron density profile in the ionospheric *F* region, *Ann. Geophys.* **15**, 314-326.

TITHERIDGE, J.E. (1998): Temperatures in the upper ionosphere and plasmasphere, *J. Geophys. Res.*, **103**, 2261-2277.

(received February 3, 1999;
accepted July 29, 1999)